Geodetic and Astrometric VLBI at K/Q/W/D Bands with the KVN

Shuangjing Xu, Taehyun Jung, Do-Young Byun

Abstract Extending geodetic and astrometric VLBI observations to millimeter (mm) wavebands offers numerous scientific possibilities and benefits. However, it was considered challenging due to various factors, including the increased effects of atmospheric opacity and turbulence. The multi-frequency system of the Korean VLBI Network (KVN) allows simultaneous observations at K/Q/W/D bands spanning 18 to 142 GHz, showing great potential for geodetic applications. We present the results of the first geodetic-mode VLBI experiment at K/Q/W/D bands (22/43/88/132 GHz). In this experiment, we introduced the Frequency Phase Transfer (FPT) method to geodetic VLBI analysis. FPT serves as an approach to calibrating atmospheric phase fluctuations at higher frequencies by transferring phase solutions from lower frequencies. This technique resulted in a higher fringe detection rate and mitigated systematic errors in delay and delay rate. Achieving weighted root-mean-squares (WRMS) of post-fit residuals at the $\sim$10 ps level with K/Q bands and $\sim$20 ps level with W/D bands demonstrates the feasibility of employing mm wavebands for high-precision geodetic applications. Additionally, we provide insights into ongoing activities and future collaborations with the Global VLBI community.

Keywords reference systems / astrometry / techniques: interferometric / quasars: general / galaxies: nuclei/radio continuum: general

Korea Astronomy and Space Science Institute, 776 Daedeok-daero, Yuseong-gu, Daejeon 34055, Republic of Korea

1 Introduction

Geodetic and astrometric Very Long Baseline Interferometry (VLBI) observations using centimeter wavebands have made significant contributions to astronomy and geodesy, particularly in the areas of the terrestrial reference frame (TRF), the celestial reference frame (CRF), and the earth orientation parameters (EOPs). The accuracy of geodetic and astrometric measurements relies on the precision of derived group delays, baseline length, and systematic delay errors. In addition to the traditional S/X band (2.3/8.4 GHz), multiple frequency bands have recently been employed. The broadband VLBI Global Observing System (VGOS) system at 2–14 GHz has improved the precision of group delays to a few picoseconds (ps); however, further efforts are required to calibrate systematic errors at the level of 20 ps originating from tropospheric delay and source structure [1, 2]. Higher frequency bands offer advantages such as achieving higher-resolution imaging of radio sources, mitigating source structure effects, measuring frequency-dependent position shifts (i.e., core-shift), and reducing interference from scattering and plasma effects. Therefore, K-band (24 GHz), X/Ka-band (8.4/32 GHz), and Q-band (43 GHz) have been used for establishing a multi-frequency CRF [3, 4].

The independent geodetic VLBI programs operating at different frequencies may have astrometric limitations in detecting the core-shift in most ICRF sources [2]. As frequency increases, VLBI fringes' SNR is affected by decreased flux densities of sources, shorter coherence times, increased atmospheric absorption, and higher receiver temperatures, limiting the precision of group delays at mm wavelengths.

The single K-band observation also has difficulty in calibrating the ionospheric delay [3].

The Korean VLBI Network (KVN) has the capability of simultaneously observing at multiple frequencies[1], including K-band at 18–26 GHz, Q-band at 35–50 GHz, W-band at 85–116 GHz, and D-band at 125–142 GHz. A similar K/Q/W-band system is being developed globally [5]. This kind of system is particularly useful for extending the coherence time at mm wavelengths using the frequency phase transfer (FPT) technology [6]. Specifically, it achieves this by calibrating the tropospheric phase at higher frequencies through transferring phase solutions from lower frequencies. This enables the observation of more sources and facilitates the measurement of core shift effects using source-frequency phase-referencing (SFPR) astrometry [6]. The global K/Q/W band system may also benefit the CRF by employing geodetic and astrometric VLBI across a broad frequency range from 20 to over 100 GHz. This approach offers several advantages:

1. overcoming limitations in group delay precision at mm wavelengths through very broad bandwidth synthesis;
2. simultaneous multi-frequency investigation of core shift effects and source structures; and
3. providing numerous ICRF source images with resolutions of a few tens of microarcseconds.

We present the first geodetic VLBI observation at 22/43/88/132 GHz simultaneously using the KVN as a pilot experiment for future broad bandwidth synthesis from 20 to over 100 GHz. Additionally, we introduce the ongoing activities.

2 Observations and Data Analysis

We conducted the first geodetic and astrometric VLBI experiment observed at 22/43/88/132 GHz simultaneously using the KVN under the East Asian VLBI Network (EAVN) program a2129a. The KVN consists of three 21-m antennas: KVN-Yonsei (KYS), KVN-Ulsan (KUS), and KVN-Tamna (KTN), with baseline lengths ranging from 305 to 476 km. We used a 24-hour track for the session from 2021-Dec-07/15:25:00 to 2021-Dec-08/15:25:00. The received signals were recorded with four 512-MHz base-band channels (BBCs) and 2 bits per sample for a total sampling rate of 8 Gbps.

[1] *https://radio.kasi.re.kr/status_report.php?cate=KVN*

We observed 82 sources, all of which were detected at K/Q/W/D bands during a KVN survey and are included in the ICRF3 K-band catalog [4]. We conducted two-minute scans for each source, scheduling a total of 485 scans for each KVN baseline.

The observations were correlated using the *DiFX* software correlator. The *HOPS* main tool, *fourfit*, was used to estimate group and phase delays, phase, delay rate, and cross-correlation amplitude for each observation. The geodetic analysis was conducted using the *nuSolve* program. Contrary to the standard practices in geodetic VLBI, we introduced the utilization of FPT to address the effects of atmospheric turbulence in mm wavebands (Xu et al. 2024, under review). We disassembled the database into individual bands (e.g., K, Q, W, D) and dual-bands (e.g., Q/K, W/K, D/K) by manually editing the *wrapper* file in the *vgosDb* database. We calculated the central frequencies of each band as the effective frequency and used these for ionospheric calibration.

Obtaining the final geodetic estimate involved a multi-step process, progressing from the least precise to the most precise corrections. This included adjustments for clock shifts and rates, station positions, ionospheric corrections for dual-frequency data, time-varying models of clock and tropospheric parameters, Earth's rotation rate, and nutation angles. The sequence of estimation, re-weighting, and outlier checks was iterated until no outliers were detected, resulting in the final solution.

3 Results

The weather conditions were clear, leading to excellent detection (SNR $\geq$ 7), with the detection rate of 99.8% at K-band, 99.8% at Q-band, 95.5% at W-band (or 96.3% with FPT), and 68.2% (or 70.9% with FPT) at D-band for 485 scans on KYS-KTN baseline. The Q-band data from the KUS station were not used due to an instrumental error.

3.1 The Group Delay and Delay Rate Measurements at 22/43/88/132 GHz

As shown in Figure 1, the FPTed phases exhibit close agreement with the trends observed in self detected phases at each K/Q/W/D bands. The clear linear phase

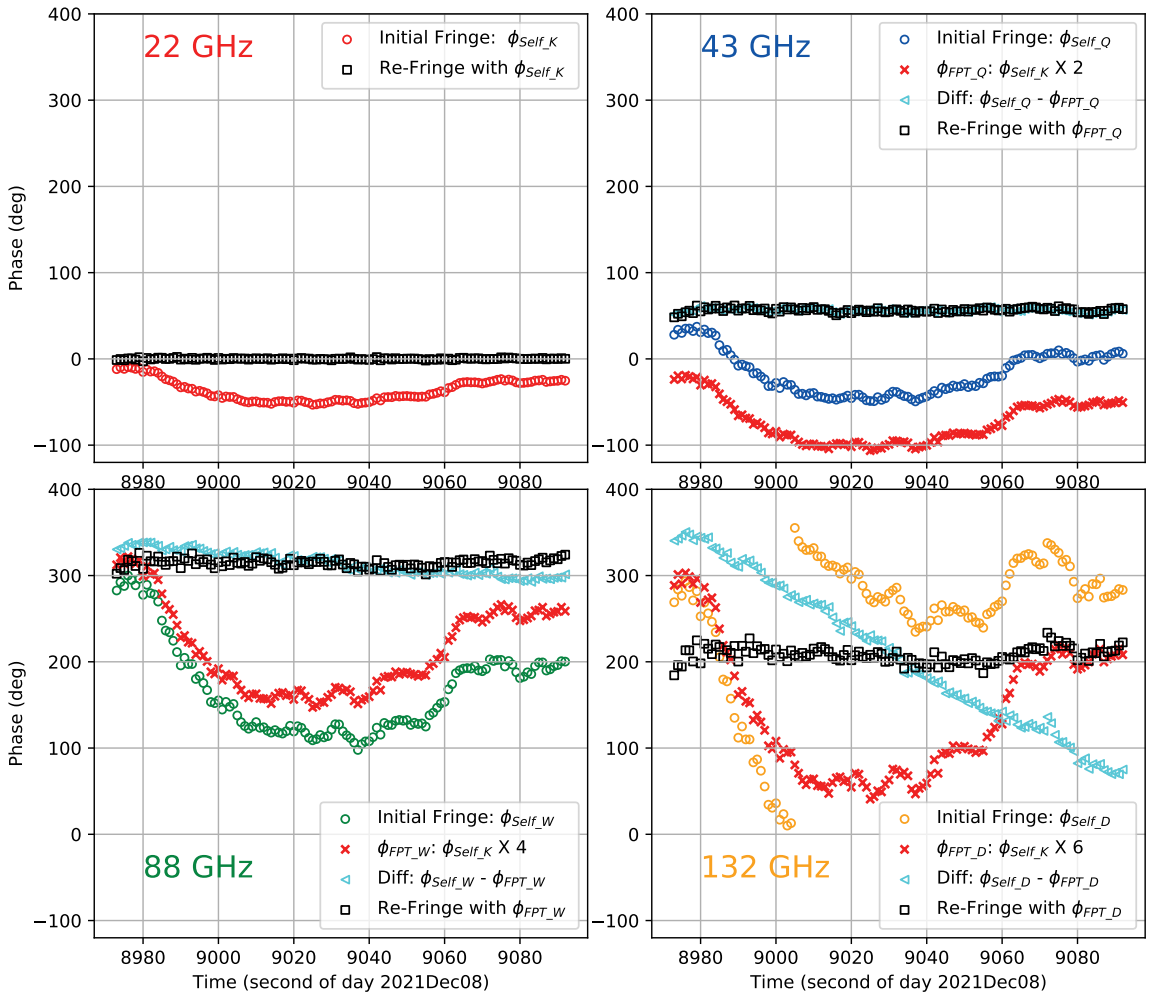

Fig. 1 Comparison of the atmospheric phase fluctuations using self detection (ϕ_{Self}) and the FPT (ϕ_{FPT}) method using the strong source 3C279 on the baseline KTN-KYS. The four panels represent distinct frequency bands.

differences (Diff: $\phi_{Self} - \phi_{FPT}$ in Figure 1) between self detection and the FPT method indicate the different delay rates. FPT improved the SNR of most fringes, some by over 100% with a two-minute scan length, resulting in a higher detection rate (over 100 observables) for weak sources at mm wavebands.

The median precision of group delays on the baseline KYS-KTN is 3.5 ps at K-band, 5.0/4.7 ps at Q-band, 22.5/19.5 ps at W-band, and 49.7/43.0 ps at D-band without/with FPT. Similarly, the median formal errors of delay rates are 6.6E-4 ps/s at K-band, 5.0E-4/4.8E-4 ps/s at Q-band, 1.1E-3/9.8E-4 ps/s at W-band, and 1.7E-3/1.5E-3 ps/s at D-band without/with FPT.

In mm wavebands, atmospheric phase fluctuations become notable within seconds, resulting in errors in fringe fitting when using a 2D linear model (phase vs. time, phase vs. frequency) over a two-minute scan duration. Consequently, uncalibrated atmospheric phase fluctuations will contribute to non-closure errors in mm wavebands. The weighted standard deviations of closure group delays are 3.7 ps at K-band, 19.9/15.7 ps at W-band, and 47.2/36.7 ps at D-band without/with FPT. Similarly, the weighted standard deviations of closure delay rates are 1.7E-3 ps/s at K-band, 3.5E-2/1.3E-3 ps/s at W-band, and 6.1E-2/1.3E-3 ps/s at D-band without/with FPT. The FPT method significantly enhances

Table 1 Geodetic results.

Band ID	Frequency (MHz)	Atmospheric phase calibration	Recoverable delays	Used delays	WRMS (ps)	chi2pdof
K	21984	NO	1447 (99.5%)	1444 (99.2%)	12.38	1.00
		ϕ_{Self_K}	1447 (99.5%)	1444 (99.2%)	12.31	1.00
Q	42620	NO	484 (99.8%)	483 (99.6%)	11.64	1.00
		ϕ_{FPT_Q}	484 (99.8%)	483 (99.6%)	11.76	1.00
W	87936	NO	1371 (94.2%)	1369 (94.1%)	25.02	1.00
		ϕ_{FPT_W}	1397 (96.0%)	1389 (95.5%)	20.46	1.00
D	131904	NO	936 (64.3%)	934 (64.2%)	39.34	1.00
		ϕ_{FPT_D}	1038 (71.3%)	1032 (70.9%)	27.56	0.99

the closure delay rate and closure phase by over an order of magnitude at W and D bands.

3.2 The Ionospheric Effects with KVN

The current work provides the greatest spanned frequency range yet used to calibrate the ionosphere. The ionospheric delays of single K-band or Q-band geodetic observations were usually calibrated using the global vertical total electron content (TEC) map derived from global navigation satellite system (GNSS) observations [3, 4]. The ionospheric delays in our KVN observations are only at the 10-picosecond level for K-band, a few picoseconds for Q-band, and less than 1 picosecond for W and D bands. The Q/W/D bands in the case of KVN are largely unaffected by ionospheric influences.

For the W and D bands, larger WRMS values are observed due to larger delay uncertainties. The utilization of either GNSS TEC maps or Q/K-band VLBI combinations did not yield noticeable improvements in WRMS, possibly attributed to the limited influence of ionospheric effects within the short baseline of KVN. Nonetheless, considering our data quality (a few ps at K- and Q-band), the Q/K-band VLBI combination holds promise for ionospheric calibration on long baselines (dozens of TECUs).

3.3 Geodetic Results

The post-fit delay residuals in Table 1 exhibit a WRMS of 12.4 ps at K-band and 11.8 ps at Q-band. When employing FPT, there is no noticeable difference in WRMS at K and Q bands. In the case of W and D bands, the visibility phases are significantly affected by atmospheric turbulence. Consequently, the WRMS of the post-fit residuals decreased from 25.0 ps to 20.5 ps at W-band and from 39.3 ps to 27.6 ps at D-band. This indicates that the errors introduced by atmospheric phase fluctuations contributing to the WRMS are $\sim$14 ps for W-band and $\sim$28 ps for D-band in this experiment.

The source positions estimated in geodetic analysis for this experiment achieve milliarcsecond precision, posing challenges in investigating sub-milliarcsecond frequency-dependent position offsets. Nevertheless, this can be achieved with multiple epochs, extended baselines, and/or including SFPR method.

4 Conclusion and Outlook

This first geodetic VLBI experiment at 22/43/88/132 GHz demonstrates that mm wavebands can be used for geodetic applications with high precision. We achieved a fringe detection rate of $\sim$ 95% at W-band and $\sim$ 70% at D-band. The WRMS values were 12.4 ps at K-band, 11.8 ps at Q-band, 20.5 ps at W-band, and 27.6 ps at D-band. We introduced the FPT method to geodetic VLBI analysis for calibrating atmospheric phase fluctuations, which improved fringe detection and enhanced the accuracy of delay measurements at the W and D bands.

The challenges regarding geodetic VLBI at the mm waveband might actually be surmountable. The number of detectable ICRF sources at K/Q/W bands is expected to surpass several hundred with KVN. In geodetic mm-VLBI scheduling, reference-pointing scans need to be developed to ensure accurate antenna pointing. The precision of group delay with

broad bandwidth synthesis from 20 to 100 GHz with KVN can be comparable to or better than VGOS, as demonstrated in a fringe in [7]. The KVN phase-cal system is undergoing testing to determine delay and phase offsets among different bands and monitor the impact of ambient temperature changes on signal chain components. The short KVN baselines limit our ability to explore the ionosphere, source structure, and frequency-dependent offsets in source positions. We are engaged in global geodetic VLBI at 86 GHz with GMVA to investigate systematic errors, extend the AGN sample at 86 GHz from KVN survey data, and determine the station coordinates of mm-VLBI antennas. We anticipate access to longer baselines with tri-band (K/Q/W) receivers in the coming years [5], enabling more comprehensive investigations.

Acknowledgements

This work utilized the KVN under the EAVN program. We are grateful to all staff members in KVN and EAVN who helped to operate the array. The KVN and a high-performance computing cluster are facilities operated by the KASI (Korea Astronomy and Space Science Institute). This research was supported by the National Research Council of Science & Technology (NST) grant by the Korea government (MSIT) (No. CAP22061-000).

References

1. M. H. Xu, J. M. Anderson, R. Heinkelmann, S. Lunz, H. Schuh, and G. Wang. Observable quality assessment of broadband very long baseline interferometry system. *Journal of Geodesy*, 95(5), doi: 10.1007/s00190-021-01496-7, 51, 2021.
2. L. Petrov. Radioastrometry at different frequencies. *arXiv e-prints*, doi: 10.48550/arXiv.2404.08800, arXiv:2404.08800, 2024.
3. G. E. Lanyi, D. A. Boboltz, P. Charlot, A. L. Fey, E. B. Fomalont, B. J. Geldzahler, D. Gordon, C. S. Jacobs, C. Ma, C. J. Naudet, J. D. Romney, O. J. Sovers, and L. D. Zhang. The Celestial Reference Frame at 24 and 43 GHz. I. Astrometry. *AJ*, 139(5), doi: 10.1088/0004-6256/139/5/1695, 1695–1712, 2010.
4. P. Charlot, C. S. Jacobs, D. Gordon, S. Lambert, A. de Witt, J. Böhm, A. L. Fey, R. Heinkelmann, E. Skurikhina, O. Titov, E. F. Arias, S. Bolotin, G. Bourda, C. Ma, Z. Malkin, A. Nothnagel, D. Mayer, D. S. MacMillan, T. Nilsson, and R. Gaume. The third realization of the International Celestial Reference Frame by very long baseline interferometry. *A&A*, 644 doi: 10.1051/0004-6361/202038368, A159, 2020.
5. R. Dodson, C. García-Miró, M. Giroletti, T. Jung, M. Lindqvist, A. Lobanov, M. Rioja, E. Ros, T. Savolainen, B. W. Sohn, A. Zensus, and G.-Y. Zhao. Radio Astronomy with Multiband Receivers and Frequency Phase Transfer: Scientific Perspectives. *arXiv e-prints*, doi: 10.48550/arXiv.2306.04516, arXiv:2306.04516, 2023.
6. M. J. Rioja and R. Dodson. Precise radio astrometry and new developments for the next-generation of instruments. *A&ARv*, 28(1), doi: 10.1007/s00159-020-00126-z, 6, 2020.
7. S. Xu, T. Jung, and D.-Y. Byun, Geodetic and Astrometric VLBI at K/Q/W/D Bands with the KVN, Zenodo, doi:10.5281/zenodo.10902979, 2024.